Mechanism of EF-Ts-Catalyzed Guanine Nucleotide Exchange in EF-Tu: Contribution of Interactions Mediated by Helix B of EF-Tu†

Tobias Schümmer, Kirill B. Gromadski, and Marina V. Rodnina*

Institute of Physical Biochemistry, University of Witten/Herdecke, D-58448 Witten, Germany

Received December 3, 2006; Revised Manuscript Received February 16, 2007

ABSTRACT: Elongation factor Tu (EF-Tu) belongs to the family of GTP-binding proteins and requires elongation factor Ts (EF-Ts) for nucleotide exchange. Crystal structures suggested that one of the salient features in the EF-Tu·EF-Ts complex is a conformation change in the switch II region of EF-Tu that is initiated by intrusion of Phe81 of EF-Ts between His84 and His118 of EF-Tu and may result in a destabilization of Mg^{2+} coordination and guanine nucleotide release. In the present paper, the contribution of His84 to nucleotide release was studied by pre-steady-state kinetic analysis of nucleotide exchange in mutant EF-Tu in which His84 was replaced by Ala. Both intrinsic and EF-Ts-catalyzed nucleotide release was affected by the mutation, resulting in a 10-fold faster spontaneous GDP release and a 4-fold faster EF-Ts-catalyzed release of GTP and GDP. Removal of Mg^{2+} from the EF-Tu·EF-Ts complex increased the rate constant of GDP release 2-fold, suggesting a small contribution to nucleotide exchange. Together with published data on the effects of mutations interfering with other putative interactions between EF-Tu and EF-Ts, the results suggest that each of the contacts in the EF-Tu·EF-Ts complex alone contributes moderately to nucleotide destabilization, but together they act synergistically to bring about the overall 60000-fold acceleration of nucleotide exchange in EF-Tu by EF-Ts.

Elongation factor Tu (EF-Tu) is a GTPase that plays an essential role during the elongation phase of protein synthesis. EF-Tu in a complex with GTP delivers aminoacyl-tRNA to the ribosome where the GTPase of EF-Tu is activated. After GTP hydrolysis and release of aminoacyl-tRNA, EF-Tu·GDP dissociates from the ribosome. EF-Tu has a higher affinity for GDP ($K_d \approx 10^{-9}$ M) than for GTP ($K_d \approx 10^{-8}$ M), and the spontaneous dissociation of GDP from EF-Tu is too slow ($0.002\ s^{-1}$) to be physiologically relevant (*1*, *2*). Recycling of EF-Tu·GDP to EF-Tu·GTP is catalyzed by the guanine-nucleotide exchange factor (GEF) EF-Ts. EF-Ts binds to EF-Tu·GDP to form the EF-Tu·GDP·EF-Ts complex (Figure 1A), which is unstable and rapidly releases GDP. Subsequent binding of GTP leads to the EF-Tu·GTP·EF-Ts complex which, in turn, dissociates into EF-Ts and EF-Tu·GTP, yielding the active form of the factor. EF-Ts enhances the dissociation of GDP from EF-Tu by a factor of 60000, which is sufficient to sustain rapid protein synthesis in vivo (*2*).

EF-Tu is a globular protein that folds into three domains. As all members of the GTPase superfamily, EF-Tu has a GDP/GTP-binding domain, domain 1 or G domain, which changes conformation in a switch-like fashion (*3*, *4*). Crystal structures indicated that EF-Tu undergoes a substantial structural rearrangement when switching between the active (GTP bound) and the inactive (GDP bound) state (*5*−*10*). The transition involves secondary structure changes in domain 1 and a large-scale change in the orientation of domain 1 relative to domains 2 and 3 (*9*). The switch from the GTP- to the GDP-bound form of EF-Tu involves conformational changes in two parts of the G domain: the switch I region (residues 40−62) and the switch II region which consists of helix B (residues 84−92) and the flanking loops (*8*).

In the EF-Tu·EF-Ts complex, the overall shape of EF-Tu is similar to that of the GDP-bound state (*11*−*13*). In the complex, EF-Ts interacts with domains 1 and 3 of EF-Tu. Mutational analysis demonstrated that the interactions of the G domain of EF-Tu with the N-terminal domain and subdomain N of EF-Ts are essential for nucleotide dissociation, whereas the contacts between the G domain of EF-Tu and the C-terminal module of EF-Ts (helix 13) and between domain 3 of EF-Tu and subdomain C of EF-Ts are less important (*14*). Structural and kinetic analyses suggested that several interactions contribute to nucleotide exchange (Figure 1B,C). First, EF-Ts induces a movement of helix D of the EF-Tu G domain that shifts Lys136 and Asp138 of EF-Tu, which are involved in the stabilization of the ribose and the guanine base, away from the nucleotide binding site, thereby relaxing the interactions of those residues with the ribose and/or guanine base (*11*, *15*). Second, Phe81 of EF-Ts, a residue in the conserved TDFV sequence motif of EF-Ts, intrudes between two histidine residues in domain 1 of EF-Tu, His84 in helix B (switch II region) and His118 in helix C. The comparison of the crystal structures of EF-Tu·EF-Ts and EF-Tu·GDP suggested that the displacement of His118 disrupts the binding of the β-phosphate of GDP, due to the successive displacement of Gln114, His19, and Val20, of which the latter two belong to the phosphate-binding loop

†This work was supported by the Deutsche Forschungsgemeinschaft, the Alfried Krupp von Bohlen und Halbach-Stiftung, and the Fonds der Chemischen Industrie.

* Corresponding author: tel, +49 2302 926205; e-mail, rodnina@uni-wh.de.

10.1021/bi602486c CCC: $37.00
Published on Web 03/31/2007

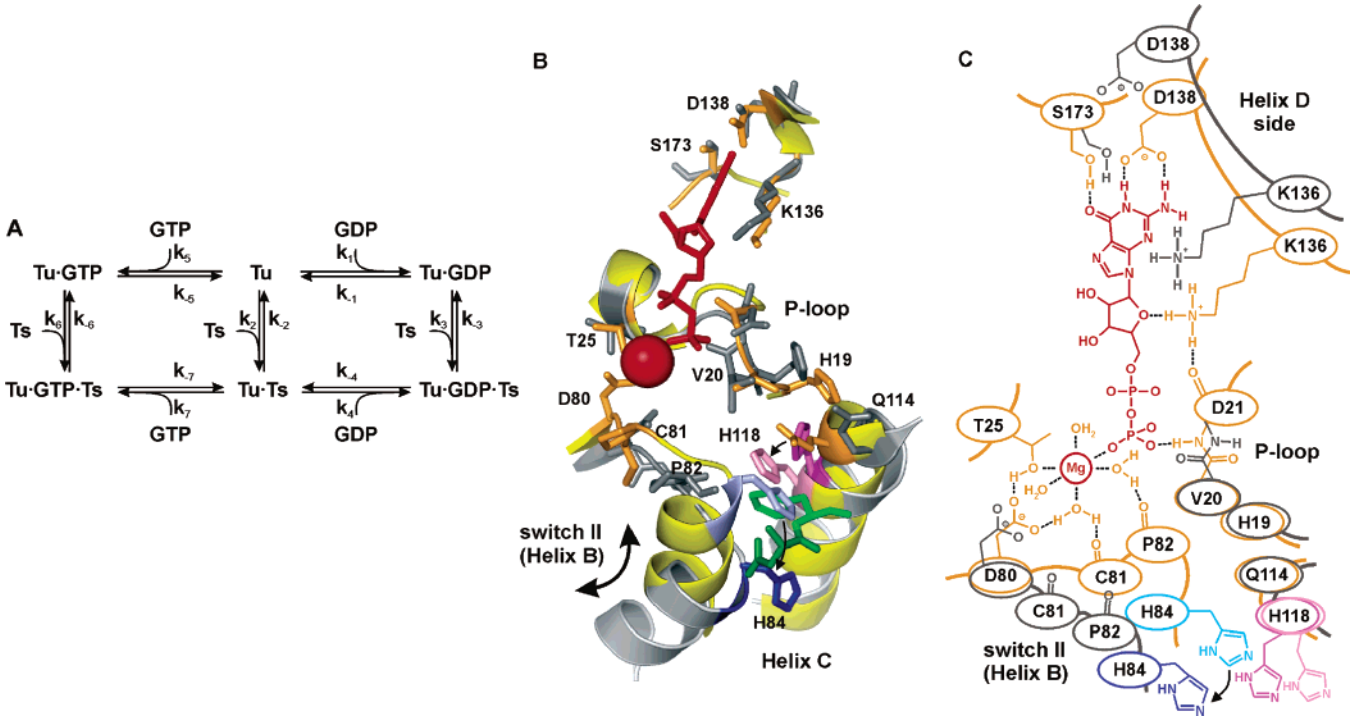

FIGURE 1: Nucleotide exchange in EF-Tu. (A) Kinetic mechanism. (B) Orientation of EF-Tu in EF-Tu·GDP (yellow) or EF-Tu·EF-Ts (gray) complexes. Residues important for nucleotide exchange are highlighted in orange and dark gray. His84 is shown in light blue in EF-Tu·GDP and dark blue in EF-Tu·EF-Ts; His118 is shown in dark lilac (EF-Tu·GDP) and light lilac (EF-Tu·EF-Ts). Phe81 of EF-Ts is shown in light green and Asp80 in dark green. GDP and the coordinated Mg^{2+} ion are indicated in red. The figure was prepared by using coordinates 1EFC and 1EFU in the Protein Data Bank (*8*, *11*). (C) Schematic representation of the nucleotide binding pocket of EF-Tu in the complex with GDP or EF-Ts using the same color code as in (B).

(P-loop) of EF-Tu. The displacement of Val20 causes a flip in the backbone of the P-loop that breaks the hydrogen bond to the β-phosphate (*11*−*13*). The importance of Phe81 of EF-Ts as well as of His118 and Val20 of EF-Tu for nucleotide exchange was demonstrated previously (*16*−*18*). The intrusion of Phe81 of EF-Ts also shifts the position of helix B of EF-Tu. The shifted position of helix B appears to be stabilized by the conserved Asp80 of EF-Ts that interacts with the amino terminus of helix B at the main-chain imino groups of His84, Ala85, and Asp86, the latter interaction being mediated by a water molecule (*11*). The movement of helix B alters the position of the strand containing Asp80, Cys81, and Pro82 of EF-Tu which are involved in the stabilization of water molecules coordinating the Mg^{2+} ion in the EF-Tu·GDP complex; kinetic measurements suggested that the loss of Mg^{2+} promotes the dissociation of GDP up to 300-fold (*2*), probably due to repulsion of the β-phosphate (Figure 1B,C).

The importance of the switch II region of EF-Tu for both nucleotide binding and factor function on the ribosome is well documented. Two conserved Gly residues 83 and 94, which are flanking helix B, are important for the binding of the ternary EF-Tu·GTP·aa-tRNA complex to the ribosome, the structural transition from the GTP- to the GDP-bound form after GTP hydrolysis, and for the dissociation of EF-Tu·GDP from the ribosome (*19*−*21*). The substitution of Gly94 with Ala in EF-Tu resulted in a conformation that favored the binding of GTP (*22*). In contrast, the exchange of Gln97 by Pro decreased spontaneous GDP release and GTP binding about 2−3-fold, while the addition of EF-Ts restored the wild-type rate of GDP release (*23*). EF-Ts mutants in which Asp80 and Phe81, which contact the switch II region of EF-Tu, were replaced with Ala were 2−3-fold less active in promoting GDP release, compared to wild-type EF-Ts, and the double mutant was nearly 10-fold less active (*17*); the effect of these mutations on the elemental kinetic steps of nucleotide exchange was not studied in detail. On the other hand, the replacement with Ala of His118 in EF-Tu, which is believed to move upon intrusion of Phe81 of EF-Ts into EF-Tu, resulted in a much larger inhibition of EF-Ts-dependent nucleotide release from EF-Tu than did the replacement of Phe81 in EF-Ts (Figure 1B).

His84 is located in the middle of the switch II region of EF-Tu. It is directly involved in the interactions with EF-Ts via Asp80 and assumes significantly different orientations in the EF-Tu complexes with GDP and EF-Ts (Figure 1B) (*11*). It is not known whether this reflects an essential function of His84 in nucleotide exchange. On the other hand, His84 is crucial for GTP hydrolysis by EF-Tu on the ribosome (*24*). The catalytic role of His84 suggested by the kinetic analysis of the EF-Tu(H84A) mutant is to stabilize the GTPase transition state by hydrogen bonding to the γ-phosphate of GTP or to the attacking water molecule.

Here we have studied the importance of His84 in EF-Tu by a kinetic analysis of the spontaneous and EF-Ts-catalyzed nucleotide exchange in the EF-Tu(H84A) mutant. The kinetics of the elemental reactions (Figure 1A) was solved using experimental approaches described previously for wild-type EF-Tu (*2*). The kinetic effects of the replacements of His84 (this paper) and His188 (*18*) and of mutations in helix D of EF-Tu (*15*) are compared to estimate the contributions of different contacts to the overall kinetics of nucleotide exchange.

MATERIALS AND METHODS

Buffer and Reagents. Experiments were performed in buffer A (50 mM Tris-HCl, pH 7.5, 70 mM NH_4Cl, 30 mM KCl, 10 mM $MgCl_2$) at 20 °C. Chemicals were purchased from Roche Biochemicals or Merck. Fluorescent mant-GDP was from Molecular Probes or JenaBioScience.

Expression and Purification of Proteins. The plasmid construct for the expression of EF-Ts as a fusion protein containing an intein self-splicing element and a chitin binding domain in the IMPACT I system (NE Biolabs) was provided by Charlotte Knudsen (Aarhus). EF-Ts was purified to homogeneity as described (*2*, *15*). EF-Ts concentrations were determined by absorbance at 210 nm (*25*) and 205 nm (*26*).

EF-Tu(H84A) and wild-type EF-Tu with a C-terminal oligohistidine tag were expressed and purified to homogeneity as described (*24*). The concentration of EF-Tu was determined photometrically at 280 nm using a molar extinction coefficient of 32900 M^{-1} cm^{-1} (*27*). As EF-Tu forms a tight complex with EF-Ts [$K_d = 3$ nM (*2*)] in the absence of nucleotide, the presence of GDP during the purification was essential to avoid the contamination of EF-Tu preparations with EF-Ts, which was verified as described (*18*). Briefly, EF-Ts-free EF-Tu was preincubated with mant-GDP, and the complex was rapidly mixed with an excess of unlabeled GDP in the stopped-flow apparatus. The release of the bound mant-GDP from the EF-Tu·mant-GDP complex was monitored by a decrease of the mant-GDP fluorescence which was excited by fluorescence resonance energy transfer (FRET) from Trp184 of EF-Tu. In the absence of EF-Ts, the release is very slow, 0.002 s^{-1} (*2*). If a given preparation of EF-Tu(H84A) is free of EF-Ts, its addition together with GDP to the EF-Tu·mant-GDP complex does not affect the rate of mant-GDP release. If, in contrast, traces of EF-Ts were present in the test sample, the rate of mant-GDP dissociation from the wild-type EF-Tu was increased significantly. According to this test, all EF-Tu preparations used in the present work were free of EF-Ts traces.

Nucleotide-free EF-Tu was prepared as described (*2*, *15*). In order to remove Mg^{2+} and allow GDP dissociation, EF-Tu was incubated in buffer A without Mg^{2+} and with 15 mM EDTA for 20 min at 37 °C. The protein was purified by gel filtration on a Superdex 75 HR column (Pharmacia) in buffer A without Mg^{2+} and was immediately used in the stopped-flow experiments. Nucleotide-free EF-Tu obtained by this procedure was stable and had the same properties as untreated EF-Tu with respect to interactions with EF-Ts and guanine nucleotides (*2*). The EF-Tu·EF-Ts complex was obtaining by mixing EF-Tu and EF-Ts in equimolar amounts for 30 min at 37 °C, purified by gel filtration in buffer A, and immediately used in stopped-flow experiments. To obtain the EF-Tu·mant-GDP/mant-GTP complexes, EF-Tu·GDP was incubated with a 5-fold excess of mant-GDP or mant-GTP and purified on either a NAP-10 column (Amersham Pharmacia Biotech) or a Superdex 75 HR column (Pharmacia).

Rapid Kinetic Measurements. The interactions of EF-Tu with guanine nucleotides and EF-Ts were studied essentially as described (*2*, *15*, *18*). Fluorescence stopped-flow measurements were performed on a SX-18MV spectrometer (Applied Photophysics) in buffer A at 20 °C. The interaction between EF-Tu and EF-Ts was monitored by the fluorescence change of Trp184 of EF-Tu (*28*). Trp fluorescence was excited at 280 nm and measured after passing cutoff filters (KV335, Schott). The fluorescence of mant-GDP was excited either via FRET from Trp, excited at 280 nm, or directly at 349 nm and measured after passing cutoff filters (KV408, Schott). Experiments were performed by rapidly mixing equal volumes (60 μL each) of the reactants and monitoring the fluorescence change over time. Time courses depicted in the figures were obtained by averaging 5−10 individual transients. Data were evaluated by fitting the exponential function $F = F_\infty + A \exp(-k_{app}t)$, with a characteristic time constant, k_{app}, the amplitude of the signal change, A, the final signal, F_∞, and the fluorescence at time t, F. Calculations were performed using TableCurve software (Jandel Scientific) or Prism (Graphpad Software). The amplitude of the fluorescence change of mant-GDP was up to 20% when FRET excitation was used and 15% for direct excitation; the fluorescence change of Trp184 was 5%. Standard deviations of apparent rate constants, k_{app}, were calculated using the same software. All elemental rate constants of nucleotide exchange, except k_{-2}, were measured directly. The value of k_{-2} was estimated from all other rate constants according to the model depicted in Figure 1A. Standard deviations of rate constants were estimated from the variation of values obtained in different experiments.

RESULTS

Kinetic Model of Nucleotide Exchange. The kinetic scheme of nucleotide exchange on EF-Tu is shown in Figure 1A. EF-Tu can bind GDP (association rate constant k_1), GTP (k_5), or EF-Ts (k_2) to form the respective binary complexes, which dissociate with the rate constants k_{-1}, k_{-5}, and k_{-2}, respectively. The interaction of EF-Tu·GDP or EF-Tu·GTP with EF-Ts can be described by two consecutive equilibria that represent the formation of the unstable ternary complex and nucleotide release, respectively. EF-Ts interacts with EF-Tu·GDP to form the ternary complex EF-Tu·GDP·EF-Ts (association and dissociation rate constants k_3 and k_{-3}, respectively). GDP is released from the ternary complex to form the binary complex EF-Tu·EF-Ts (k_{-4}); the reaction is reversible (k_4). By analogy, EF-Tu·GTP can bind EF-Ts (k_6), and the ternary complex can dissociate into either EF-Tu·GTP and EF-Ts (k_{-6}) or EF-Tu·EF-Ts and GTP (k_{-7}). The binding of GTP to the binary EF-Tu·EF-Ts complex is characterized by k_7. Note that the rate constants k_1, k_2, k_3, k_4, k_5, k_6, and k_7 are bimolecular association rate constants (M^{-1} s^{-1}), whereas the rate constants k_{-1}, k_{-2}, k_{-3}, k_{-4}, k_{-5}, k_{-6}, and k_{-7} are monomolecular dissociation rate constants (s^{-1}).

Interaction of GDP/GTP and EF-Ts with Nucleotide-Free EF-Tu (k_1, k_{-1}, k_2, k_5, k_{-5}). The interaction of EF-Tu with guanine nucleotides was studied essentially as described (*2*, *15*, *18*). The experiments were carried out with wild-type and mutant EF-Tu; as the rate constants obtained with the wild-type factor were identical to those published previously (*2*, *15*, *18*), only the results obtained with EF-Tu(H84A) are described in the following. To measure the association rate constants k_1 and k_5, a constant amount of nucleotide-free EF-Tu(H84A) was titrated with mant-GDP/mant-GTP (Figure 2A), monitoring the fluorescence of mant-GDP or mant-GTP excited by FRET (Materials and Methods). Apparent rate constants, k_{app}, obtained by single-exponential

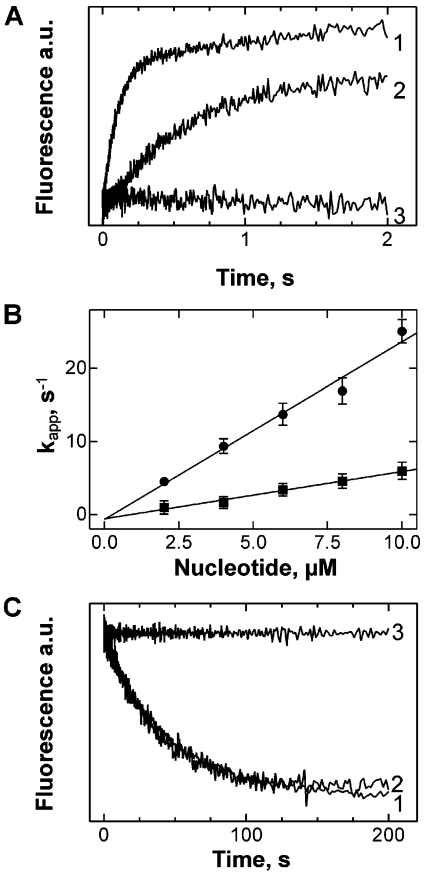

FIGURE 2: Interaction of mant nucleotides with EF-Tu(H84A) in the absence of EF-Ts. (A) Time courses of (1) mant-GDP (3 μM) or (2) mant-GTP (3 μM) binding to nucleotide-free EF-Tu (0.5 μM); (3) control without EF-Tu. Fluorescence of mant was excited by FRET from Trp in EF-Tu. (B) Concentration dependence of k_{app} of binding. Values of k_{app} for mant-GDP (circles) or mant-GTP (squares) were calculated by exponential fitting of the time courses, examples of which are shown in (A). (C) Release of mant-GTP (1) or mant-GDP (2) from EF-Tu·mant-GDP or EF-Tu·mant-GTP (0.1 μM) in the presence of excess unlabeled nucleotide (25 μM); (3) control with EF-Tu·mant-GDP (0.1 μM) in the absence of GDP.

fitting were plotted against nucleotide concentration (Figure 2B), yielding straight lines with slopes corresponding to k_1 or k_5; the values of the association rate constants were very similar to those reported for the wild-type EF-Tu (*2*) (Table 1). The intercept with the *Y*-axis was close to zero for both nucleotides, and thus the value of k_{-1} and k_{-5} could not be determined with precision in these experiments. The rate constants of nucleotide release from EF-Tu(H84A)·mant-GDP (k_{-1}) and EF-Tu(H84A)·mant-GTP (k_{-5}) were determined in the presence of excess unlabeled GDP/GTP using direct mant excitation (Figure 2C). In this case, the rate by which the fluorescence decreases reflects the dissociation rate constant of mant-GDP/mant-GTP from EF-Tu, because in the presence of a large excess of unlabeled nucleotide, rebinding of labeled nucleotide is negligible. The rate constant of mant-GDP release (k_{-1}) from EF-Tu(H84A) was 0.023 ± 0.003 s^{-1}, 10-fold higher than observed with wild-type EF-Tu [0.002 s^{-1} (*2*)]. The difference in the rate constants was also observed when mant-GDP release from EF-Tu(H84A) and the wild-type protein was compared side by side in a single experiment. The rate constant of GTP dissociation (k_{-5}) 0.03 ± 0.005 s^{-1} from EF-Tu(H84A) was the same as with the wild-type protein.

Table 1: Effect of Mutations in EF-Tu on Rate Constants of EF-Tu Interactions with EF-Ts and Nucleotides

rate constant[a]	wt[b]	H84A	H118A[c]	E152A[b]
k_1, 10^6 M^{-1} s^{-1}	2	2.4	3.5	2.0
k_{-1}, s^{-1}	0.002	0.023	0.03	0.003
k_2, 10^7 M^{-1} s^{-1}	1	3.4		0.08
k_{-2}, s^{-1}	0.03	0.06[d]	nd	0.04
k_3, 10^7 M^{-1} s^{-1}	6	5.5	7	0.46
k_{-3}, s^{-1}	350	190	280	170
k_4, 10^7 M^{-1} s^{-1}	1.4	1.2	0.5	0.76
k_{-4}, s^{-1}	125	520	2.3	9
k_5, 10^5 M^{-1} s^{-1}	5	6.4	2.5	
k_{-5}, s^{-1}	0.03	0.03	0.2	nd
k_6, 10^7 M^{-1} s^{-1}	3	5	9	
k_{-6}, s^{-1}	60	74	120	nd
k_7, 10^6 M^{-1} s^{-1}	6	4.7	0.4	
k_{-7}, s^{-1}	85	350	4.4	nd

[a] According to the mechanism of Figure 1. Standard deviations of constants are 5−20%. [b] From ref *15*. [c] From ref *18*. [d] Average between 0.03 and 0.09 s^{-1} calculated from the GDP and GTP cycles, respectively.

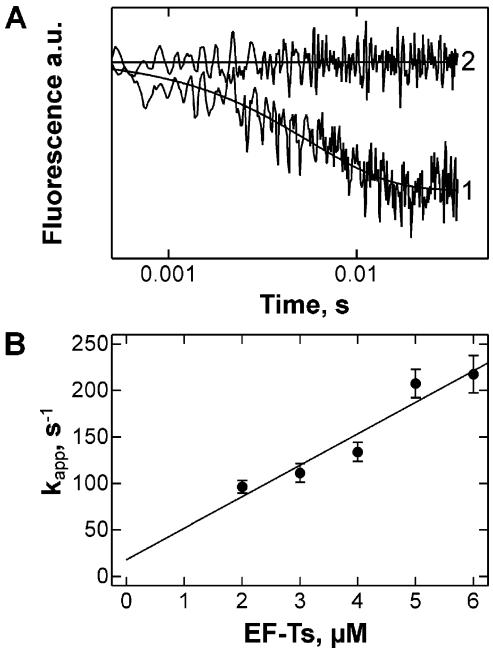

FIGURE 3: EF-Tu(H84A)·EF-Ts interactions. (A) Time courses of (1) EF-Ts (5 μM) binding to nucleotide-free EF-Tu(H84A) (1 μM) and (2) control in the absence of EF-Ts. The fluorescence of Trp184 in EF-Tu was monitored. (B) Concentration dependence of k_{app} of EF-Tu(H84A)·EF-Ts complex formation.

Rate constants of EF-Ts binding to nucleotide-free EF-Tu(H84A) were measured by monitoring Trp fluorescence. To determine the association rate constant, time courses were measured at increasing concentrations of EF-Ts (Figure 3A), and the value of k_2 was determined from the slope of the linear concentration dependence of k_{app} (Figure 3B). The value of the association rate constant of EF-Tu with EF-Ts was $k_2 = (3.4 \pm 0.6) \times 10^7$ M^{-1} s^{-1} for the H84A mutant and $(1.1 \pm 0.2) \times 10^7$ M^{-1} s^{-1} for wild type (Table 1), suggesting that the rate of EF-Ts binding was moderately affected by mutation. The intercept with the *Y*-axis was close to zero, and thus k_{-2} could not be determined with precision.

Interaction of EF-Tu(H84A) with EF-Ts in the Presence of GDP (k_3, k_{-3}, k_4, k_{-4}) or GTP (k_6, k_{-6}, k_7, k_{-7}). To measure the rate constant of EF-Ts-catalyzed GDP release, k_{-4}, a constant amount of EF-Tu(H84A)·mant-GDP was titrated

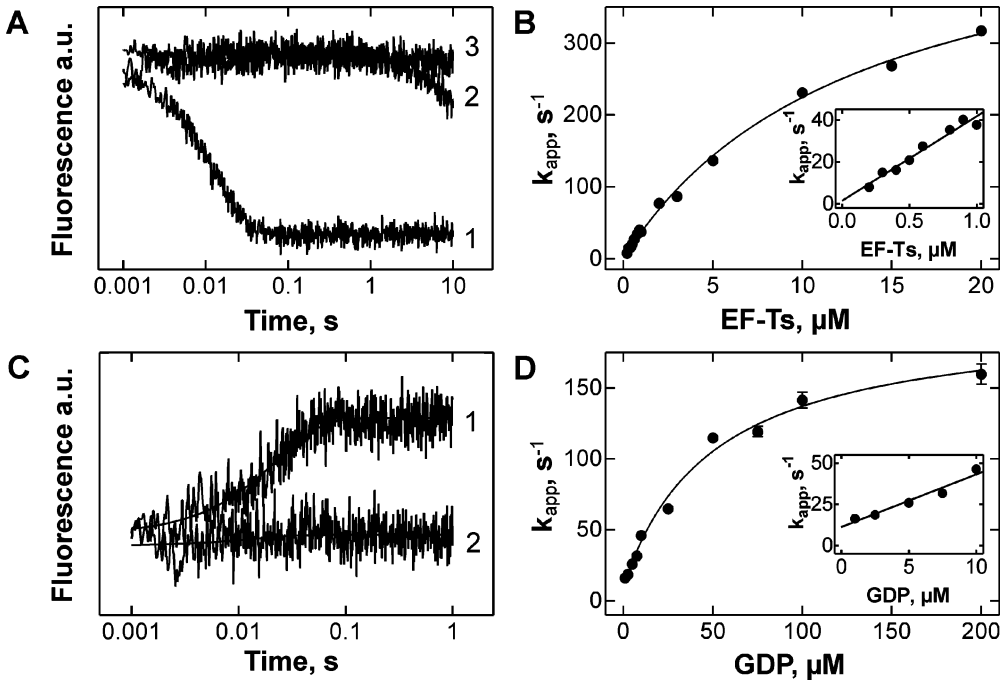

FIGURE 4: Interaction of EF-Tu(H84A) with EF-Ts and GDP. (A) Time course of dissociation of EF-Tu(H84A)·mant-GDP (0.1 μM) in the presence of EF-Ts (2 μM) and excess unlabeled GDP (25 μM) (1), in the absence of EF-Ts (2), or in the absence of EF-Ts and unlabeled GDP (3) measured by direct excitation of mant fluorescence. (B) Concentration dependence of k_{app}. Values of k_{app} were calculated by single-exponential fitting from the time courses as shown in (A). The inset here and in the following figures shows the initial part of the curve. (C) Time course of dissociation of EF-Tu(H84A)·EF-Ts (0.5 μM) in the presence of GDP (10 μM) (1) or in the absence of the nucleotide (2). Fluorescence of Trp184 in EF-Tu was monitored. (D) Concentration dependence of k_{app}. The values of k_{app} were calculated by single-exponential fitting from the time courses as shown in (C).

with increasing amounts of EF-Ts, monitoring the fluorescence of the mant group upon direct excitation. An excess of unlabeled GDP was added together with EF-Ts, in order to avoid rebinding of mant-GDP. Single-exponential fluorescence decay was observed which was attributed to the dissociation of mant-GDP (Figure 4A). Apparent rate constants of mant-GDP release were plotted against increasing EF-Ts concentration. At low concentration of the EF-Ts, k_{app} increased linearly, indicating that the association of EF-Ts with EF-Tu(H84A)·mant-GDP was rate limiting (Figure 4B); thus, the initial slope of the titration curve (Figure 4B, inset) is equal to $k_3/(1 + k_{-3}/k_{-4})$ (*29*), and the value of k_3 can be calculated, provided k_{-4} and k_{-3} are known.

At high concentration of EF-Ts, the release of GDP from the EF-Tu(H84A)·GDP·EF-Ts complex is rate limiting, and the apparent rate constant at saturation equals k_{-4}. Fitting a hyperbolic function resulted in a value of $k_{-4} = 520 \pm 30$ s^{-1} (compared to 150 s^{-1} for wild-type EF-Tu) (Table 1). To determine k_{-3}, titrations were carried out with a fixed concentration of the purified EF-Tu(H84A)·EF-Ts complex and increasing concentrations of GDP. Trp fluorescence was monitored which reflects the binding of EF-Tu to EF-Ts and is insensitive to nucleotide binding (*2*). Upon mixing EF-Tu(H84A)·EF-Ts with GDP, a single-exponential fluorescence increase was observed due to the dissociation of EF-Ts (Figure 4C). Apparent rate constants of EF-Ts dissociation were plotted against the nucleotide concentration (Figure 4D). Fitting the data to a hyperbolic function yielded a saturation value of 190 ± 20 s^{-1}, which corresponds to k_{-3} (compared to 350 s^{-1} for wild-type EF-Tu) (Table 1). The contribution of the reverse reaction, i.e., the rebinding of EF-Ts to the EF-Tu(H84A)·GDP complex, given by k_3[EF-Ts], is negligible at saturating concentrations of GDP, because the concentration of free EF-Ts does not exceed the initial concentration of the EF-Tu(H84A)·EF-Ts complex, 0.5 μM. The initial slope of the titration curve (Figure 4D, inset) is given by $k_4/(1 + k_{-4}/k_{-3})$ and thus yielded the rate constant of the association of GDP to the EF-Tu(H84A)·EF-Ts complex [$k_4 = (1.2 \pm 0.5) \times 10^7$ M^{-1} s^{-1}] (Table 1). Thus, the values of k_3 and k_4 measured with EF-Tu(H84A) are close to those reported for wild-type EF-Tu (*2*, *15*), whereas the values of k_{-3} and k_{-4} are about 2-fold lower and 4-fold higher, respectively.

The interactions between EF-Tu(H84A), EF-Ts, and GTP were studied in the same way as described above for GDP, except that GTP solutions were preincubated with phosphoenolpyruvate and pyruvate kinase in order to convert any GDP to GTP (Figure 5, Table 1). The values of k_6, k_{-6}, and k_7 were not significantly different with the mutant compared to the wild-type EF-Tu, and k_{-7} was the only rate constant that was affected by the H84A mutation [350 s^{-1} compared to 85 s^{-1} with wild-type EF-Tu (*2*)].

Calculation of k_{-2}. The rate constant of EF-Tu(H84A)·EF-Ts dissociation was the only constant which could not be measured directly and was therefore calculated from other rate constants on the basis of the law of mass action. From the rate constants of the right [$k_{-2} = k_{-1}k_2k_{-3}k_4/(k_1k_3k_{-4})$] and left [$k_{-2} = k_{-5}k_2k_{-6}k_7/(k_5k_6k_{-7})$] part of the scheme in Figure 1A, values for k_{-2} were calculated as 0.03 and 0.09 s^{-1} for GDP and GTP, respectively, yielding an average value of $k_{-2} = 0.06$ s^{-1}, which is the same as the value of ~0.03 s^{-1} reported previously for wild-type EF-Tu (*2*, *15*), given the standard deviations of the rate constants used for the calculation.

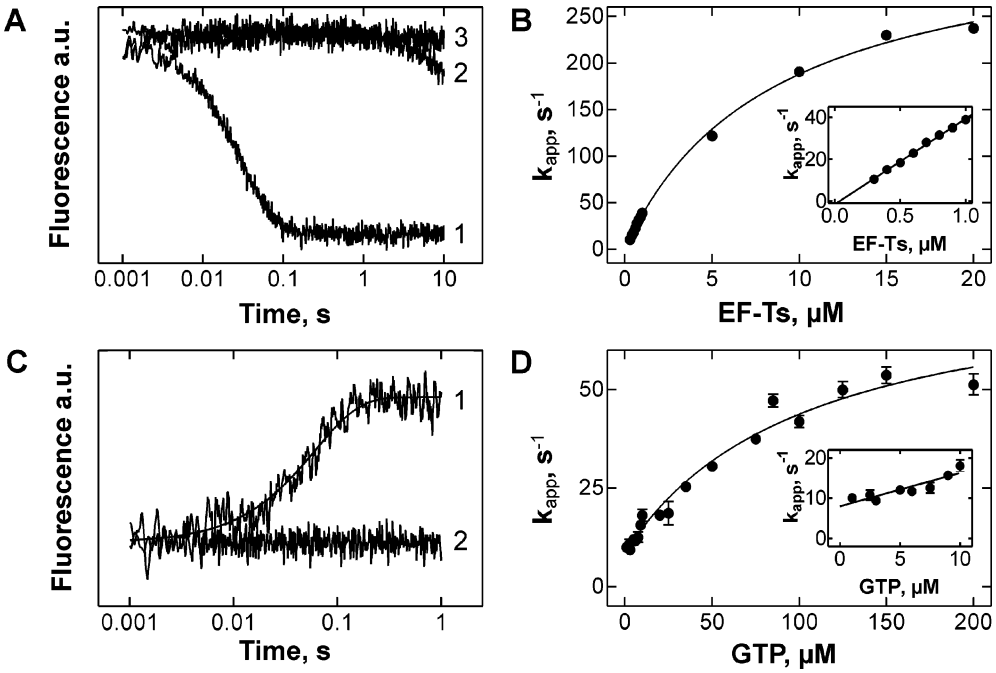

FIGURE 5: Interaction of EF-Tu(H84A) with EF-Ts and GTP. (A) Time course of dissociation of EF-Tu(H84A)·mant-GTP (0.1 μM) in the presence of EF-Ts (0.7 μM) and excess unlabeled GTP (25 μM) (1), in the absence of EF-Ts (2), or in the absence of EF-Ts and unlabeled GDP (3) measured by direct excitation of mant fluorescence. GTP and mant-GTP solutions were preincubated with phosphoenolpyruvate and pyruvate kinase to eliminate contaminating GDP. (B) Concentration dependence of k_{app}. (C) Time course of the dissociation of EF-Tu(H84A)·EF-Ts (0.5 μM) in the presence of GTP (20 μM) (1) or in the absence of the nucleotide (2). Fluorescence of Trp184 in EF-Tu was monitored. (D) Concentration dependence of k_{app}.

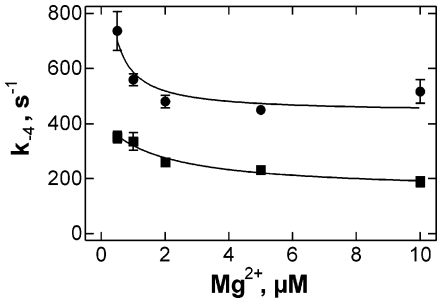

FIGURE 6: Mg^{2+} dependence of GDP release from EF-Tu·GDP·EF-Ts. Values for k_{-4} obtained from the saturation of the concentration dependencies of k_{app} (Figure 4B) were determined at different Mg^{2+} concentrations. Key: wild-type EF-Tu (squares); EF-Tu(H84A) (circles).

GDP Dissociation at Different Mg^{2+} Concentrations. To study the contribution of Mg^{2+} coordination to GDP binding in the presence of EF-Ts, we measured dissociation of the EF-Tu(H84A)·GDP·EF-Ts complex (k_{-4}) in the presence of different Mg^{2+} concentrations (Figure 6). k_{-4} was determined at saturation of EF-Ts. The rate constants of GDP dissociation from both EF-Tu(H84A)·GDP·EF-Ts and EF-Tu·GDP·EF-Ts increased up to 2-fold with decreasing Mg^{2+}. At all Mg^{2+} concentrations the rate of GDP dissociation was about 2 times faster with EF-Tu(H84A) compared to wild-type EF-Tu. Thus the effect of the mutation on the dissociation of GDP was independent of Mg^{2+}, at least in the concentration range of Mg^{2+} studied in these experiments.

DISCUSSION

Effects of the His84Ala Mutation on Nucleotide Exchange in EF-Tu. The mutation of His84 in EF-Tu affects several steps in the mechanism of nucleotide exchange (Table 1). The rate constants of spontaneous GDP dissociation (k_{-1}) and EF-Ts-stimulated release of GDP (k_{-4}) and GTP (k_{-7}) are increased by a factor of 4−10, whereas the rate of GTP dissociation (k_{-5}) was not changed. The effect of the mutation on the rate of spontaneous GDP dissociation must be indirect, as His84 does not interact with the nucleotide (*5*−*8*). The overall fold of EF-Tu(H84) must be correct, because the mutant retains its ability to interact efficiently with EF-Ts (this paper), aminoacyl-tRNA, and the ribosome (*24*). In the GTP-bound form of EF-Tu, helix B spans residues 83−93, and the main-chain imino groups of Gly83 and His84 and the carbonyl group of Thr61 coordinate the hydrolytic water molecule (*9*, *10*); as the side chain of His84 is not involved and points outward to the solvent, the H84A mutation may have no effect on the stability of the EF-Tu·GTP complex. In the GDP-form of EF-Tu, the position of helix B is shifted, and His84 is found in close proximity to His118 and Glu117 and may be involved in the stabilization of the contacts between helices B and C (*5*−*8*). The H84A replacement may render the packing less tight and more prone to dynamic rearrangements, hence the increase of the dissociation constant for GDP. In comparison, the mutation of His118 in EF-Tu, a residue located close to His84 but far from the nucleotide binding pocket, was shown to increase the release rates of both GDP and GTP (*18*). The effect was attributed to the loss of His118 interactions with Gly18 in the P-loop or a more general effect of the mutations on the structure of the subunit interface, both resulting in weaker nucleotide binding.

Crystal structures suggest that one of the key interactions between EF-Tu and EF-Ts entails the insertion of the Phe81 side chain of EF-Ts into a hydrophobic pocket in EF-Tu formed by His84, His 118, and Leu121 (*11*, *12*). Thus, one may expect that replacement of His84 should diminish the ability of EF-Tu to bind EF-Ts. This is, however, not the

case, because the association rate constants for EF-Ts were either not changed (k_3) or even slightly increased (k_2, k_6) by the H84A mutation (Table 1). This small increase may be explained by the removal of the bulky side chain of His84, which in wild-type EF-Tu may create a steric challenge for EF-Ts binding and require additional time for mutual conformational adjustments at the contact interface.

It can be expected that the removal of a residue involved in an EF-Ts-induced shift of helix B that eventually disrupts the coordination of the Mg^{2+} ion (*11*, *12*) should decrease the rate of EF-Ts-catalyzed nucleotide release, assuming that the loss of Mg^{2+} is an important requisite for nucleotide release and that the contact between Phe81 of EF-Ts and His84 of EF-Tu initiated the rearrangement. However, in contrast to this expectation, the rate constants of GTP and GDP dissociation from the EF-Tu(H84A)·EF-Ts complex were increased, rather than decreased (Table 1). One possible explanation is that the mutation affects the position of helix B in the complex, which may destabilize Mg^{2+} coordination even more than in wild-type EF-Tu. However, if this were the case, one would expect different Mg^{2+} dependencies of the GDP dissociation rate for mutant and wild-type EF-Tu. Specifically, if Mg^{2+} binding were additionally destabilized by the mutation, more Mg^{2+} should be required to decrease the dissociation rate constant in EF-Tu(H84A)·EF-Ts compared to the wild-type complex. As this does not appear to be the case (Figure 6), it is more likely that the overall organization of the Mg^{2+} binding pocket of EF-Tu in the complex with EF-Ts is not disturbed by the mutation and the increase in the nucleotide dissociation rates is due to other factors. These may involve indirect effects caused by disturbed helix B−helix C interactions, including an influence of the H84A mutation on the interaction between Phe81 of EF-Ts with His118 of EF-Tu, a changed interface between domains 1 and 3, and an increased mobility of the switch II region.

Critical Interactions between EF-Tu and EF-Ts. Three factors may contribute to the nucleotide exchange: (1) disruption of the Mg^{2+} binding site in the G domain of EF-Tu, (2) a rearrangement in the P-loop of EF-Tu that causes an altered binding of the phosphate moieties of GDP/GTP, and (3) a relaxation of interactions with the ribose and/or guanine base. Structural studies suggested that the changes in Mg^{2+} coordinaton and in the P-loop are initiated by insertion of Phe81 of EF-Ts between helices B and C of EF-Tu, whereas the interactions between the N-terminal domain of EF-Ts and helix D of EF-Tu destabilize the interactions of residues of EF-Tu with the ribose and the guanine base (*11*, *12*). The contribution to nucleotide exchange and timing of these events cannot be established by structural approaches and requires a quantitative analysis of the interactions between EF-Tu, EF-Ts, and the nucleotides and the effect of mutations of key residues. The results of such quantitative mutational analysis (refs *2*, *14*, *15*, *17*, and *18* and this paper) can be summarized as follows.

The formation of the contacts between helix D of EF-Tu and the N-terminal domain of EF-Ts is the rate-limiting step for binding, as mutations in helix D, but not in helices B or C, reduced the rate constant of EF-Ts binding to EF-Tu by a factor of 10 (*15*). Contacts involving helices B and C of EF-Tu seem to be established later and to be rapid compared to the preceding bimolecular binding step (*2*, *15*). Furthermore, mutations in helix D of EF-Tu reduced the rate of nucleotide dissociation from the EF-Tu·EF-Ts complex by a factor of 10 (e.g., the E152A mutation in EF-Tu). Thus, helix D provides a key interaction during both the early step of EF-Ts binding and the following nucleotide release, which indicates that the interactions of the base side of the nucleotide are disturbed first, followed by the rearrangements at the phosphate side of the nucleotide (*15*).

In contrast to the contacts through helix D of EF-Tu, the interactions induced by the intrusion of Phe81 of EF-Ts are important only for nucleotide dissociation, as mutations of both His84 (this work) or His118 (*18*) had practically no effect on the binding of EF-Ts to EF-Tu. Mutations of Asp80 and Phe81 of EF-Ts resulted in a 2−3-fold slower nucleotide release (*17*), and mutation of His84 of EF-Tu increased the rate of nucleotide dissociation (this work). These effects are rather small compared to the overall 60000-fold acceleration of nucleotide exchange in EF-Tu by EF-Ts (*2*). On the other hand, His118 appears to be important, as mutations of His118 resulted in a 60-fold decrease of the rate constant of GDP dissociation (*18*). Given the small effects of mutations of Asp80 and Phe81 of EF-Ts, the large inhibitory effect of the His118 mutations on the nucleotide dissociation is unexpected and suggests that other EF-Tu-EF-Ts contacts, in addition to the Phe81 intrusion, contribute to the nucleotide exchange.

The role of destabilization and loss of the Mg^{2+} ion to the mechanism of nucleotide exchange is of particular interest. In the absence of EF-Ts, removal of Mg^{2+} accounts for a 150−300-fold acceleration of GDP dissociation. In the presence of EF-Ts, Mg^{2+} also influences the rate of nucleotide dissociation, but the effect is only 2-fold (Figure 6). This suggests that, although nucleotide release is faster in the absence of Mg^{2+} (*11*, *12*), binding of Mg^{2+} to EF-Tu·EF-Ts does not render the complex inactive. Thus, the loss of Mg^{2+} has a very limited contribution to EF-Ts-catalyzed nucleotide release. In summary, disruption of any of the putative key interactions in the EF-Tu·EF-Ts complex resulted in only small to moderate changes in the efficiency of nucleotide exchange. It is possible that, in addition to the salient changes indicated by the crystal structures (*11*, *12*), EF-Ts binding induces many small rearrangements of EF-Tu that contribute synergistically to efficient exchange of guanine nucleotides.

ACKNOWLEDGMENT

We thank C. Knudsen (Aarhus University) for providing the plasmid coding for the EF-Ts-intein construct, C. Pohl for help in the preparation of Figure 1B, and P. Striebeck, A. Böhm, C. Schillings, and S. Möbitz for expert technical assistance.

REFERENCES

1. Wagner, A., Simon, I., Sprinzl, M., and Goody, R. S. (1995) *Biochemistry 34*, 12535−12542.
2. Gromadski, K. B., Wieden, H. J., and Rodnina, M. V. (2002) *Biochemistry 41*, 162−169.
3. Kjeldgaard, M., Nyborg, J., and Clark, B. F. (1996) *FASEB J. 10*, 1347−1368.
4. Vetter, I. R., and Wittinghofer, A. (2001) *Science 294*, 1299−1304.
5. Kjeldgaard, M., and Nyborg, J. (1992) *J. Mol. Biol. 223*, 721−742.

6. Polekhina, G., Thirup, S., Kjeldgaard, M., Nissen, P., Lippmann, C., and Nyborg, J. (1996) *Structure 4*, 1141−1151.
7. Abel, K., Yoder, M. D., Hilgenfeld, R., and Jurnak, F. (1996) *Structure 4*, 1153−1159.
8. Song, H., Parsons, M. R., Rowsell, S., Leonard, G., and Phillips, S. E. (1999) *J. Mol. Biol. 285*, 1245−1256.
9. Kjeldgaard, M., Nissen, P., Thirup, S., and Nyborg, J. (1993) *Structure 1*, 35−50.
10. Berchtold, H., Reshetnikova, L., Reiser, C. O., Schirmer, N. K., Sprinzl, M., and Hilgenfeld, R. (1993) *Nature 365*, 126−132.
11. Kawashima, T., Berthet-Colominas, C., Wulff, M., Cusack, S., and Leberman, R. (1996) *Nature 379*, 511−518.
12. Wang, Y., Jiang, Y. X., Meyering-Voss, M., Sprinzl, M., and Sigler, P. B. (1997) *Nat. Struct. Biol. 4*, 650−656.
13. Jeppesen, M. G., Navratil, T., Spremulli, L. L., and Nyborg, J. (2005) *J. Biol. Chem. 280*, 5071−5081.
14. Zhang, Y., Yu, N.-J., and Spremulli, L. L. (1998) *J. Biol. Chem. 273*, 4556−4562.
15. Wieden, H. J., Gromadski, K., Rodnin, D., and Rodnina, M. V. (2002) *J. Biol. Chem. 277*, 6032−6036.
16. Jacquet, E., and Parmeggiani, A. (1988) *EMBO J. 7*, 2861−2867.
17. Zhang, Y., Li, X., and Spremulli, L. L. (1996) *FEBS Lett. 391*, 330−332.
18. Dahl, L. D., Wieden, H. J., Rodnina, M. V., and Knudsen, C. R. (2006) *J. Biol. Chem. 281*, 21139−21146.
19. Kjaersgard, I. V., Knudsen, C. R., and Wiborg, O. (1995) *Eur. J. Biochem. 228*, 184−190.
20. Knudsen, C., Wieden, H. J., and Rodnina, M. V. (2001) *J. Biol. Chem. 276*, 22183−22190.
21. Kothe, U., and Rodnina, M. V. (2006) *Biochemistry 45*, 12767−12774.
22. Knudsen, C. R., Kjaersgard, I. V., Wiborg, O., and Clark, B. F. (1995) *Eur. J. Biochem. 228*, 176−183.
23. Navratil, T., and Spremulli, L. L. (2003) *Biochemistry 42*, 13587−13595.
24. Daviter, T., Wieden, H. J., and Rodnina, M. V. (2003) *J. Mol. Biol.* 332, 689−699.
25. Tombs, M. P., Souter, F., and Maclagan, N. F. (1959) *Biochem. J. 73*, 167−171.
26. Scopes, R. K. (1974) *Anal. Biochem. 59*, 277−282.
27. Block, W., and Pingoud, A. (1981) *Anal. Biochem. 114*, 112−117.
28. Jameson, D. M., Gratton, E., and Eccleston, J. F. (1987) *Biochemistry 26*, 3894−3901.
29. Fersht, A. (1999) *Structure and mechanism in protein science*, W. H. Freeman, New York.

BI602486C